Published in final edited form as:
Neuroscience. 2010 September 1; 169(3): 1186–1198. doi:10.1016/j.neuroscience.2010.05.073.

The basolateral amygdala differentially regulates conditioned neural responses within the nucleus accumbens core and shell

Joshua L. Jones[1], **Jeremy J. Day**[1], **Robert A. Wheeler**[1], and **Regina M. Carelli**[1,2]

[1]Department of Psychology, University of North Carolina at Chapel Hill, Chapel Hill, North Carolina 27599

[2]Neuroscience Center, University of North Carolina at Chapel Hill, Chapel Hill, North Carolina 27599

Abstract

The ability to process information regarding reward-predictive cues involves a diverse network of neural substrates. Given the importance of the nucleus accumbens (NAc) and the basolateral amygdala (BLA) in associative reward processes, recent research has examined the functional importance of BLA-NAc interactions. Here, multi-neuron extracellular recordings of NAc neurons coupled to microinfusion of $GABA_A$ and $GABA_B$ agonists into the BLA were employed to determine the functional contribution of the BLA to phasic neural activity across the NAc core and shell during a cued-instrumental task. NAc neural response profiles prior to BLA inactivation exhibited largely indistinguishable activity across the core and shell. However, for NAc neurons that displayed cue-related increases in firing rates during the task, BLA inactivation significantly reduced this activity selectively in the core (not shell). Additionally, phasic increases in firing rate in the core (not shell) immediately following the lever press response were also significantly reduced following BLA manipulation. Concurrent with these neural changes, BLA inactivation caused a significant increase in latency to respond for rewards and a decrease in the percentage of trials in which animals made a conditioned approach to the cue. Together, these results suggest that an excitatory projection from the BLA provides a selective contribution to conditioned neural excitations of NAc core neurons during a cued-instrumental task, providing insight into the underlying neural circuitry that mediates responding to reward-predictive cues.

Keywords

ventral striatum; electrophysiology; reward; cue; learning; reinforcement

The nucleus accumbens (NAc) has long been described as an important neural substrate for reward processing, particularly in mediating the effects of motivationally relevant stimuli on goal-directed responding (Cardinal et al., 2002, Nicola, 2007, Humphries and Prescott, 2009). The NAc is a heterogeneous structure, primarily comprised of two anatomically and functionally distinct subregions, the core and shell (Brog et al., 1993). Both of these structures are involved in appetitive reward behaviors, though numerous studies have attributed differential functional roles of the core and shell in conditioned reinforcement (Parkinson et al., 1999), action-outcome contingencies (Corbit et al., 2001), and extinction and reinstatement (Fuchs et al., 2004). Correspondingly, NAc neuronal activity appears to track goal-directed responses (Peoples et al., 1997, Carelli, 2004, Nicola, 2007, Roesch et al., 2009) and cue-reward associations (Carelli, 2000, Setlow et al., 2003, Nicola et al.,

Corresponding author: Regina M. Carelli, Professor & Director, Behavioral Neuroscience Program, Department of Psychology, University of North Carolina, Chapel Hill, CB#3270 Davie Hall, Chapel Hill, NC 27599, rcarelli@unc.edu, (919) 962-8775.

2004a, Day et al., 2006, Hollander and Carelli, 2007). Despite clear dissociations in core and shell function, few differences in neural activity across subregions have been identified, specifically during reward-related behaviors (Ghitza et al., 2004, Hollander and Carelli, 2007). However, regional differences in NAc cell firing may be more readily apparent through circuit-level analysis (e.g., examination of the role of specific NAc afferents on NAc activity).

One critical input that has received increasing attention regarding its role in reward processing is the basolateral amygdala (BLA) (Everitt et al., 2000, Murray, 2007). Importantly, electrophysiological studies have revealed that BLA neurons are responsive to reward-predictive cues (Tye et al.,, Carelli et al., 2003, Saddoris et al., 2005, Paton et al., 2006, Tye and Janak, 2007, Ambroggi et al., 2008). Recent hypotheses suggest that the BLA is critical for maintaining the assigned value of conditioned stimuli, and using this information to guide subsequent behavior in the absence of rewards (Cardinal et al., 2002). Specifically, disruption of BLA activity does not alter instrumental conditioning (Balleine et al., 2003) or simple Pavlovian autoshaping (Parkinson et al., 2000). However, intact BLA function is necessary for the formation of a conditioned place preference (Everitt et al., 1991, McDonald and White, 1993), Pavlovian-to-Instrumental Transfer (Corbit and Balleine, 2005), cue-induced reinstatement (Fuchs et al., 2006, McLaughlin and Floresco, 2007), second-order conditioning (Everitt et al., 1989, Setlow et al., 2002a), reward devaluation (Ostlund and Balleine, 2008, Johnson et al., 2009), and responding on high effort tasks (Ghods-Sharifi et al., 2009, Simmons and Neill, 2009).

Given the essential involvement of both the NAc and the BLA in incentive reward processes, a functional link of amygalo-striatal interactions has been proposed (Everitt et al., 1999). Neurophysiological evidence has shown that stimulation of BLA efferents evoke excitatory responses in NAc neurons (O'Donnell and Grace, 1995, Floresco et al., 2001, Charara and Grace, 2003, Ambroggi et al., 2008, McGinty and Grace, 2008), and BLA activity can regulate phasic dopamine release within the NAc core (Jones et al., 2009). Indeed, the functional connectivity of the BLA-NAc pathway is necessary for animals to respond on a second-order conditioning task with a natural (Setlow et al., 2002b) or drug reinforcer (Di Ciano and Everitt, 2004). Additionally, recent evidence has shown that stimulus-controlled instrumental responding is also attenuated as a result of BLA-NAc disconnection (Ambroggi et al., 2008), as well as high effort fixed-ratio instrumental responding (Simmons and Neill, 2009).

Here, we used multi-unit extracellular electrophysiology of NAc activity coupled to microinfusion of $GABA_A$ and $GABA_B$ agonists (muscimol 0.03 nmol and baclofen 0.3 nmol in 0.3μL) (McFarland and Kalivas, 2001) into the BLA, to determine the functional contribution of the BLA to phasic neural activity across the NAc core and shell during a cued-instrumental task. Similar to previous reports, NAc neural response profiles across the core and shell exhibited largely indistinguishable activity. However, distinct subsets of NAc neurons were differentially regulated by BLA activity, specifically subsets that correlated with presentation of conditioned cues. These results provide a critical characterization of afferent modulation by the BLA of phasic signaling in the NAc core and shell.

Experimental Procedures

Animals

Male Sprague Dawley rats (90-120 d old; Harlan, Indianapolis, IN) were used (n = 12). Rats had *ad libitum* access to water, with restricted food (Laboratory Rodent Diet; PMI Nutrition International, Branson, MO) limited to 15-25g per day to maintain weight between 85-95% of pre-surgical body weight. This regimen was in place for the duration of behavioral

testing, except during the postoperative recovery period when food was given *ad libitum*. All procedures were approved by the University of North Carolina Institutional Animal Care and Use Committee.

Surgery

Animals were anesthetized with ketamine hydrochloride (100 mg/kg) and xylazine hydrochloride (20 mg/kg), and microelectrode arrays were implanted in the NAc using established procedures (Carelli et al., 2000). Electrodes were custom-designed and purchased from a commercial source (NB Laboratories, Dennison, TX, USA). Each array consisted of eight microwires (50 μm diameter) arranged in a 2x4 bundle that measured ~ 1.5 mm anteroposterior and ~ 0.75 mm mediolateral. Arrays were targeted for permanent, bilateral placement in the core and shell subregions of the NAc (AP, +1.3 to 1.7 mm relative to bregma; ML, ± 0.8 or 1.3 mm relative to bregma; DV, -6.2 mm from brain surface; (Paxinos and Watson, 2005)). Ground wires for each array were coiled around skull screws and placed into the ipsilateral side of the brain. Initially, rats (n=3) were implanted with unilateral guide cannula aimed at the BLA (anteriorposterior: -2.7 to -3.0; mediolateral: +/-4.9 from bregma; dorsoventral: -6.2 from skull, (Paxinos and Watson, 2005)). To increase the yield of data from each animal, bilateral guide cannula were implanted in the remaining rats (n=9). BLA guide cannula consisted of a 22 gauge thin-walled stainless-steel tubing (Plastics One Inc., Roanoke, VA) and were lowered to 2 mm above the target site. The cannula and microarrays were secured with stainless steel screws and dental acrylic. Stylets (Plastics One Inc., Roanoke, VA) were inserted into the length of the guide cannula to maintain patency.

Electrophysiological recordings

Electrophysiology procedures have been described previously (Carelli et al., 2000). Briefly, before the start of each session, subjects were connected to a flexible recording cable attached to a commutator that allowed virtually unrestrained movement within the chamber. NAc activity was recorded differentially between the active and the inactive electrodes from the permanently implanted microwires. On-line isolation and discrimination of neuronal activity was accomplished using a neurophysiological system commercially available (MAP system; SIG board filtering, 250 Hz to 8 kHz; sampling rate, 40 kHz; Plexon, Dallas, TX). Individual waveforms corresponding to a single cell were discriminated using template analysis procedures provided by the MAP system and sorted further after each experiment using principal component analysis in Offline Sorter (Plexon, Dallas, TX). Raster displays and perievent histograms (PEHs) were constructed using commercially available software (NeuroExplorer; Plexon, Dallas, TX).

Apparatus

Experimental sessions occurred in 43 × 43 × 53 cm Plexiglas chambers (Medical Associates, St. Albans, VT, USA) housed within sound-attenuating boxes (Medical Associates, St. Albans, VT, USA). Two symmetrically located retractable levers (Colburn Instruments, Allentown, PA, USA) were placed 17 cm apart on one wall of the chamber. Cue lights were positioned above each lever. A food receptacle was centered between the levers, 2.5 cm from the floor. A house light was centrally located on the wall opposite the food receptacle and levers, 2 cm from the ceiling.

Behavioral Task

Rats were trained to respond for sucrose (45 mg pellets; Test Diet) delivered into a receptacle on a discriminative stimulus fixed-ratio 1 (FR1) schedule of reinforcement. Sessions were limited to 90 pellets/day in a single daily session. Each training session was

initiated by the onset of the houselight, presentation of continuous white noise, and insertion of the inactive lever. Responses on the inactive lever had no programmed consequences. During the operant training session, either the discriminative stimulus (DS) or non-associated stimulus (NS) was presented on a variable-interval schedule with an average inter-trial interval of 20s. A schematic of the behavioral task is shown in Figure 1a. The DS and NS were semi-randomly presented over three trials with a 2:1 ratio of DS:NS frequency. The DS consisted of a unique audio tone (either 1000 or 2750 Hz; counterbalanced across animals) presented for 6s. Upon termination of the tone, the active lever was inserted into the chamber and the associated cue-light was illuminated. An instrumental response on the active lever resulted in lever retraction, cue-light termination and delivery of sucrose into the receptacle, as well as an additional unique 6s audio tone (8000 Hz; CS). If the rat did not respond on the active lever within 30s of presentation, the cue-light was terminated and the lever was retracted, and a new inter-trial interval was initiated. The NS consisted of the alternative tone (1000 or 2750 Hz) and was also presented for 6s. Responses during the NS had no programmed consequences. Rats underwent 10-13 days of training until criterion was met with accurate responses made on greater than 95% of DS trials across 3 consecutive sessions.

Experimental test day and microinfusion

Once trained, all rats underwent surgical procedures described above. Following recovery, animals had 5 additional operant training days. On the final two re-training days, rats were tethered and the session was divided into pre and post segments to acclimate each animal to the test day procedure, and mock microinfusions were given. On the experimental test day, NAc cell firing was recorded during a session that consisted of 135 total trials (90 DS and 45 NS; described above), divided into the pre-infusion (PRE) and post-infusion (POST) periods. After the initial 45 pre-infusion trials rats were given a 0.3μL unilateral microinfusion of either vehicle (0.9% NaCl sterile saline; VEH) or drug (0.3nmol baclofen $GABA_B$ agonist/0.03nmol muscimol $GABA_A$ agonist, in 0.9% NaCl sterile saline; BM; dose from (McFarland and Kalivas, 2001)) into one BLA cannula. Microinfusions were made over 1 min, and the injector remained in place for a 1 min post-injection diffusion period. All 12 rats received at least 2 test days, with unilateral injection of either VEH or BM. The 9 rats with bilateral cannula also received 2 additional test days in the alternate unilateral cannula. In all cases, the order of treatment was randomly assigned for each animal (alternating infusion side between days). After the microinfusion, the animals were immediately reconnected to the recording apparatus and placed in the chamber, and post-infusion trials commenced 5 min later.

Behavioral analysis

Several behavioral measures were examined: the DS and NS approach response ratios, the DS response latency, and the number of overall responses on the active and inactive levers. Approach responses were analyzed through video analyses, wherein an approach was defined as a directed movement or orienting of the animals head into the active lever region of the chamber (2in. × 2in. around the lever), during the DS or NS presentation. Response latency and lever presses were recorded via computer.

Neural analysis

NAc neuronal firing patterns were characterized using raster displays and peri-event histograms (PEHs) constructed with commercially available software (NeuroExplorer, Littleton, MA, Plexon, Dallas, TX). Raster displays and PEHs display the activity of each cell time-locked to particular behavioral events. For each cell, PEHs were constructed time-locked to either the DS, NS or operant response. To examine neural activity relative to DS presentation, cell firing was displayed during 0-1s following DS onset compared to the ‘DS

baseline' period, (−5 to 0 s prior to DS presentation). To determine neural activity relative to NS presentation cell firing was examined during the 0-1s following NS onset compared to the 'NS baseline' period (−5 to 0 s prior to NS presentation). To evaluate cell firing before and following the lever press response, cell firing was examined during the 1s period preceding the operant response (−1 - 0 pre-response) and 1s following the response (0 - 1 post-response) compared to baseline activity (the DS baseline period was used since no events occurred during that time). Next, 99.9% confidence intervals (CI) were projected in each PEH from the baseline epochs for each neuron (Neuroexplorer). Neural responses were characterized as phasic by the presence of at least one bin (beginning within each event epoch) that showed an increase or decrease in firing rate over the projected baseline CI. A subset of cells exhibited larger variability in their baseline firing rates and the projected 99.9% CI included zero. For these neurons to be classified as phasic, $e_0 > 2\ b_0$ had to be true (where e_0=consecutive zero bins occurring within the event epoch, and b_0= maximal number of consecutive zero bins in the baseline epoch).

Next, each NAc neuron was classified into specific response profiles (types), as follows. Cells that increased their firing rate in the 1s following cue-onset were classified as DSe or NSe, according to the respective cue. For cells that increased their firing rate surrounding the operant response, if the increase was marked as phasic in the pre-response period, it was considered a pre-response excitation (PRe), even if this phasic increase persisted into the post-response period. Cells that increased their firing rate only in the post-response period were classified as reinforcement excitation (RFe) neurons. Note, PRe and RFe are inherently mutually exclusive, but both types of operant responses could also be classified as cue-responsive (i.e. DSe). NAc neurons that decreased their firing rate in the 1s following cue-onset were classified as DSi or NSi respectively. Cells that decreased their firing rate surrounding the operant response were classified as operant inhibitions (OPi). Again, OPi could also be classified as cue-responsive (e.g., DSe). Note, cells were classified into phasic response patterns based upon their PRE-infusion firing PEHs, and then assigned to a phasic population. Once classified, then neurons were analyzed comparing their PRE versus POST infusion firing patterns, and subsequently compared across treatments.

Two exclusion criteria were used to remove neurons that did not meet inclusion standards noted above. Cells were excluded if the baseline firing rate preceding the DS for the PRE infusion period was less than 0.2 Hz, or if the cell had fewer than 500 spikes within the entire PRE period. Cells were also removed from analysis if the baseline firing rate during the PR period exceeded 10 Hz, as these were likely not medium-spiny neurons (Berke et al., 2004). Using this approach, of the 303 units recorded across all sessions, 15 were excluded based upon the first, and 40 units were excluded based on the second criteria.

Histology

Rats were deeply anesthetized with a ketamine and xylazine mixture (100 mg/kg and 20 mg/kg, respectively) and perfused transcardially using physiological saline, 10% formalin and 3% potassium ferricyanide, and brains were removed. In order to mark the placement of electrode tips, a 13.5 μA current was passed through each microwire electrode for 5 s. To mark microinfusion sites, a brief 5 μA current was passed through injector needles placed into the guide cannula. After post-fixing and freezing, 40-μm coronal brain sections were mounted and stained with thionin. Electrode tip locations and injection sites were identified based upon anatomical organization (Paxinos and Watson, 2005).

Statistics

Analysis of behavioral data was completed using paired t-tests. To examine acquisition of the task, a two-way repeated measures ANOVAs involving session number x cue (DS v NS)

was employed. To determine the effects of BLA inactivation on cue-evoked approach behavior a two-way repeated measures ANOVA of cue (DS v NS) x treatment (VEH v BM) was employed. All ANOVAs were followed by Bonferroni *post hoc* tests as noted. Proportions and frequencies of units and wire placements across subregions were compared using Fisher's exact test (GraphPad Prism 4).

To compare differences in mean firing rate of individual response patterns across subregions, a two-way repeated measures ANOVA of epoch (baseline v signal) x subregion (core v shell) was used. To determine the effects of BLA manipulation on cell firing, PEH were constructed for each individual neuron across the PRE and POST infusion periods to compare the within-session changes in firing. Cells were grouped based on their hemispheric relation to the infusion side as well as by subregion. To examine the effects of BLA manipulation on NAc cell firing for each cell type, three-way repeated measures ANOVAs of epoch (baseline v signal) x infusion (PRE v POST) x treatment (VEH v BM) were used. Presence of a significant 3-way interaction would indicate that the effect of infusion on epoch firing rate was dependent upon treatment. Statistics were completed on the raw firing rate data presented Tables 2 and 3. However, to simplify data representation, data were normalized and collapsed across the infusion variable (POST firing rate/ PRE firing rate) in Figures 5-6. Statistics were analyzed using either Prism 4 (GraphPad) or SPSS 17.0 (SPSS).

Results

Histology

Histological verification of electrode placement across NAc subregions revealed that there was no significant difference in the distribution of wires between the core (n=76) and shell (n=94) (χ^2= 1.91; p=0.17) (Figure 1b). Likewise, sixteen micro-infusion sites were histologically confirmed to be in the BLA. Non-BLA infusion sites (n=5) and non-NAc wire placements were excluded from analysis.

Behavior

Animals learned to successfully discriminate between the active and inactive levers and reached DS responding criterion within 13 sessions. A two-way ANOVA (lever x session) revealed a significant interaction ($F_{(1,12)}$ = 27.45, p < 0.0001) across the final 8 training sessions and subsequent retraining days (Figure 2a). Bonferroni *post hoc* tests revealed that over the final 6 training sessions and all retraining days there were significantly more responses on the active than the inactive lever (p<0.001).

Unilateral inactivation of the BLA had no significant effect on the ability of the rats to perform the behavioral task ($t_{(11)}$=1.44, p=0.17; Figure 2b). To examine the effect of BLA inactivation on conditioned responses to DS or NS presentation, both the latency to respond and the percentage of trials in which animals approached the active lever region during DS presentation was determined. Compared to VEH, BM infusion caused a significant increase in the latency to respond ($t_{(11)}$=2.718, p=0.02; Figure 2c). Further, a two-way repeated measures ANOVA revealed significant main effects of treatment (VEH and BM, $F_{(1,22)}$ = 26.67, p<0.0001) and cue (DS and NS, $F_{(1,22)}$ = 201.7, p<0.0001) and a significant interaction (treatment x cue; $F_{(1,22)}$ = 12.89, p=0.0016) on the percentage of trials in which animals approached the active lever region during DS presentation (Figure 2d). Specifically, BM treatment significantly decreased the percentage of DS trials in which the animals made an approach (p < 0.01). There was no significant difference between the VEH or BM treatment in NS trial approaches (p>0.05). Together, these data demonstrate that unilateral inactivation of the BLA attenuates DS-evoked behavior.

Subregion characterization of NAc neural activity

To characterize NAc cell firing during the task, the response profiles of neurons collected from the PRE period on the initial VEH day for each animal were analyzed. A total of 126 NAc neurons were recorded from 12 rats. There was an even distribution in cell numbers across the NAc core (n=66) and shell (n=60). Moreover, there was no significant difference in the baseline (−5 to 0 s prior to DS onset) firing rate of neurons in the core (2.12 ±0.24 spikes/s) versus the shell (2.34±0.27 spikes/s; $t_{(124)}$=0.61, p=0.54).

Table 1 shows the number of neurons that exhibited a change in firing rate during the four behavioral epochs (DS, NS, Pre-response, Post-response). It is important to note that these groups are not mutually exclusive, as neurons often demonstrated multiple response patterns. As is evident in Table 1, the majority of NAc neurons exhibited phasic activity during the task. Moreover, a greater proportion of NAc core neurons exhibited at least one phasic response (57/66; 86.4%) compared to neurons in the NAc shell (42/60; 70.0%) (Fisher's exact test; p=0.03).

Cells were then assigned to specific types and further analyzed. Examples of individual NAc neurons that exhibited excitatory response profiles are shown in Figure 3. An example of a neuron that exhibited type DSe activity, characterized by significant increases in firing rate during the 1s following cue-onset, is shown in Figure 3a (increased activity highlighted in gray bar). There was no significant difference in the proportion of neurons that exhibited DSe response profiles across the core (n=12) and shell (n=7) (Fisher's exact test; p=0.33). Although DSe neurons in each subregion showed significant increases in firing rate during the signal period (i.e., 1 s following DS onset) compared to baseline (Figure 3b) a two-way repeated measures ANOVA (subregion x epoch) was used to determine whether there were differences in DSe response profiles across subregions. The ANOVA revealed a significant main effect of epoch ($F_{(1,17)}$ = 8.97, p<0.01), but not subregion ($F_{(1,17)}$ = 1.61, p=0.22), indicating the magnitude of the DSe firing rates and baselines were similar between the core and shell.

PRe neurons were characterized by significant increases in firing rate during the 1s before the operant (lever press) response. The PEH in Figure 3c shows the activity of a representative PRe neuron. The proportion of neurons that exhibited PRe response profiles were not statistically different across the core (n=18) and shell (n=8), although this did approach significance (Fisher's exact test; p=0.08). Likewise, PRe neurons in each subregion showed significant increases in firing rate during the signal period (i.e., 1 s preceding operant response) compared to baseline (Figure 3d). Additionally, the magnitude of the PRe signal and the baseline firing rate was similar across the core and shell, as a two-way repeated measures ANOVA (subregion x epoch) revealed a significant main effect of epoch ($F_{(1,24)}$ = 14.69, p<0.001), but not subregion ($F_{(1,24)}$ = 0.82, p=0.38).

RFe neurons were characterized by significant increases in firing rate during the 1s period following the response. Neurons that exhibited RFe response profiles (example shown in Figure 3e) were also similarly distributed across the core (n=15) and shell (n=15) (Fisher's exact test; p=0.84). RFe neurons showed significant increases in firing rate during the signal period compared to baseline (Figure 3f). The magnitude and baseline firing rate of RFe neurons was similar across the core and shell, as a two-way repeated measures ANOVA (subregion x epoch) revealed a significant main effect of epoch ($F_{(1,28)}$ = 54.14, p<0.0001), but not subregion ($F_{(1,28)}$ = 1.61, p=0.22).

Neurons that exhibited inhibitory response profiles relative to behavioral events were classified as follows. DSi response neurons were characterized by significant decreases in firing rate during the 1s following DS onset. An example of a representative DSi neuron is

shown in Figure 4a (gray bar), and the decline in firing rate during the signal relative to baseline periods for all DSi cells in the core and shell is shown in Figure 4b. There was no significant difference in the proportion of NAc neurons that were classified as DSi across the core (n=13) and the shell (n=11) (Fisher's exact test; p=1.0). Likewise the magnitude of the inhibition for DSi cells was similar across subregions as the two-way repeated measures ANOVA (subregion x epoch) revealed a significant main effect of epoch ($F_{(1,22)} = 15.29$, $p<0.001$), but not subregion ($F_{(1,22)} = 1.40$, $p=0.25$) (Figure 4b). OPi neurons were characterized by significant decreases in firing rate during the 2s surrounding the operant response. Figure 4a shows an example of a representative OPi neuron. The mean firing rates during the signal and baseline periods across all OPi cells in the core and shell is shown in Figure 4d. OPi response profiles were also evenly distributed across the core (n=31) and shell (n=23) (Fisher's exact test; p=0.37). Likewise, the OPi baseline and epoch signal were similar between subregions as the two-way repeated measures ANOVA (subregion x epoch) revealed a significant main effect of epoch ($F_{(1,52)} = 44.74$, $p<0.0001$), but not subregion ($F_{(1,52)} = 0.80$, $p=0.37$). Taken together, these results demonstrate a remarkable similarity in the neural response profiles of NAc neurons across the core and shell during the task.

BLA regulation of NAc phasic excitations

The primary goal of this study was to determine the contribution of BLA activity to phasic neural responses within the NAc. As noted above, the pharmacological manipulation used in this study induced a significant reduction in conditioned responses following the presentation of the DS, with no significant disruption in instrumental responding. As such, it was hypothesized that BLA inactivation would attenuate neural firing within NAc phasic excitations, specifically DS-evoked signals.

To determine if DSe responses were altered by BLA inactivation, the firing rates of DSe neurons were compared before and following BLA inactivation. An example DSe neuron recorded in the core before and after BM treatment is shown in Figure 5a. For the population of DSe cells, a three-way repeated measures ANOVA (epoch x infusion x treatment) revealed a significant interaction of epoch x infusion x treatment ($F_{(1,11)} = 7.26$, $p=0.02$; see Table 2 for all significant main and 2-way interaction effects). The 3-way interaction reveals that ipsilateral DSe neurons in the NAc core exhibited a significant reduction in the DS-evoked signal as a result of BM treatment (Figure 5b). However, there was no significant attenuation of the DSe signal in the NAc shell following BLA inactivation, with only a main effect of epoch ($F_{(1,6)} = 34.10$, $p=0.001$) and no significant interaction of epoch x infusion x treatment ($F_{(1,6)} = 0.80$, $p>0.05$) (Figure 4c; see Table 3 for all significant main and interaction effects). Importantly, this attenuation of the DSe signal was specific to neurons ipsilateral to the BLA treatment, as neither neurons in the core (epoch x infusion x treatment; $F_{(1,2)} = 3.65$, p p>0.05) or shell (epoch x infusion x treatment; $F_{(1,9)} = 1.62$, $p>0.05$) exhibited a significant change in signal when the contralateral BLA was inactivated.

Next, the effect of BLA inactivation on PRe response profiles was examined. A representative PRe neuron from the NAc core is shown in Figure 5d. For all PRe neurons in both the core (Figure 4e; Table 2) and shell (Figure 4f; Table 3), there was no significant change in signal compared to baseline firing as a function of BLA manipulation (core; epoch x infusion x treatment $F_{(1,17)} = 0.38$, $p>0.05$; shell; epoch x infusion x treatment $F_{(1,11)} = 0.31$, $p>0.05$). However, in the shell there was a significant epoch x infusion interaction ($F_{(1,11)} = 6.49$, $p=0.002$), as there was a general decrease in PRe signal following infusion of both VEH and BM. Furthermore, there was no significant change in PRe signal in neurons contralateral to the BLA manipulation in either the core or shell (core; epoch x infusion x treatment $F_{(1,11)} = 2.43$, $p>0.05$; shell; epoch x infusion x treatment $F_{(1,6)} = 0.29$, $p>0.05$).

Third, the effects of BLA inactivation on RFe response profiles were examined. A representative RFe neuron from the NAc core is shown in Figure 5g. For RFe neurons in the core, a significant reduction in the DS-evoked signal was observed following BLA inactivation (Figure. 5h; Table 2). However, this reduction in type RFe activity was not specific to BM treatment as there was not a significant three-way interaction (epoch x infusion x treatment $F_{(1,11)} = 3.12$, $p>0.05$), but a significant epoch x infusion interaction ($F_{(1,11)} = 15.49$, $p=0.002$). That is, the reduction in RFe activity was observed following both BM and VEH infusion into the BLA. Interestingly, again neurons in the shell exhibited no significant change in signal as a result of BLA manipulation (epoch x infusion x treatment $F_{(1,8)} = 1.14$, $p>0.05$), but only a main effect of epoch ($F_{(1,8)} = 16.00$, $p=0.004$) (Figure 5i; Table 3). This attenuation of RFe signal in the core, but not the shell, is also specific to ipsilateral neurons, as there was no significant change in contralateral RFe signals in either the core or shell (core; epoch x infusion x treatment $F_{(1,8)} = 1.37$, $p>0.05$; shell; epoch x infusion x treatment $F_{(1,11)} = 3.56$, $p>0.05$).

BLA regulation of NAc phasic inhibitions

For DSi neurons across both the core and shell, there was no significant change in DSi signal compared to baseline firing as a function of BLA manipulation (core; epoch x infusion x treatment $F_{(1,11)} = 0.54$, $p>0.05$; shell; epoch x infusion x treatment $F_{(1,12)} = 0.25$, $p>0.05$) (Figure 6a and b; Tables 2 and 3). Furthermore, there was no significant change in contralateral DSi signal compared to baseline firing as a result of BLA manipulation in either the core or shell (core; epoch x infusion x treatment $F_{(1,7)} = 1.29$, $p>0.05$; shell; epoch x infusion x treatment $F_{(1,11)} = 0.83$, $p>0.05$).

The effects of BLA inactivation on OPi cell firing across the core and shell was also examined. If a neuron was not phasic across the entire OPi period, only the period in which it was phasic (i.e. preOP or postOP) was evaluated. For OPi neurons in the core, there was no significant change in OPi signal as a function of BLA manipulation (epoch x infusion x treatment $F_{(1,29)} = 1.13$, $p>0.05$) (Figure 6c; Table 2). However, OPi neurons in the shell exhibited a significant change in the baseline firing rate across both BLA treatments, with a significant epoch x infusion interaction ($F_{(1,26)} = 10.06$, $p=0.004$) (Figure 6d; Table 3). Interestingly, the change in baseline firing rate was similar across VEH (78.1% of PRE) and BM (73.1% of PRE) treatments. Furthermore, there was no significant change in the contralateral DSi signals across either the core or shell (core; epoch x infusion x treatment $F_{(1,19)} = 0.35$, $p>0.05$; shell; epoch x infusion x treatment $F_{(1,21)} = 2.16$, $p>0.05$). The functional significance of this reduction in inhibitory responding is unclear, but the finding that it occurred under both VEH and BM conditions indicates that any unknown behavioral consequences of this neural profile are not uniquely dependent upon BLA activity.

Discussion

The present findings demonstrate that the BLA differentially regulates conditioned neural responses within the NAc core and shell. Specifically, DS-evoked excitations for neurons in the NAc core, but not the shell, exhibited a significant reduction in firing rate following BM inactivation of the BLA. Additionally, excitations in firing rate in the core (not shell) immediately following the lever press response (type RFe cells) were also significantly reduced following BLA manipulation. Although this significant reduction was also observed following vehicle infusion, it was more pronounced after BM treatment. Concurrent with the DSe neural change, BLA inactivation caused a significant increase in latency to respond and decrease in the percentage of DS trials in which animals made an approach response. Together, these results suggest that an excitatory projection from the BLA provides a selective contribution to conditioned neural excitations in NAc core neurons during a cued-

instrumental task, providing insight into the underlying neural circuitry that mediates responding to reward-predictive cues.

The primary finding reported here is that distinct subsets of NAc core neurons, but not shell neurons, are regulated by BLA activity during the task. Recent evidence demonstrated that BLA activity facilitates incentive cue responses of NAc core neurons, concomitant with a decrease in stimulus-controlled behavior (Ambroggi et al., 2008). However, that study was restricted to neural activity within the NAc core. Here, both core and shell neural responses were examined. Despite similarities in neural response profiles between these subregions prior to pharmacological manipulation of the BLA, BLA inactivation differentially mediates DS-evoked excitations in the NAc core. As noted above, we also examined neural activity surrounding the operant response, and show that post-response excitations within the core were also attenuated by BLA inactivation, although not significantly more than following VEH treatment. Given the small number of RFe neurons it is possible this is a function of statistical power. Such post-response excitations have typically been associated with encoding of the CS (i.e., a distinct cue paired with reward delivery) (Carelli and Deadwyler, 1997, Carelli, 2000). We did not explicitly test this possibility with non-contingent CS probes, but it is likely that these responses encode aspects of the conditioned stimulus (Carelli and Deadwyler, 1997), the consummatory response (Nicola et al., 2004b) or reinforcer palatability (Taha and Fields, 2005). Given that the NAc core has been shown to exhibit more phasic excitations in response to a CS that evokes conditioned approaches (Day et al., 2006), it is likely that the attenuated post-response signal found here is a similar subset of CS-responsive core neurons. Taken together, these data suggest that BLA activity drives conditioned phasic excitations within the core, but not the shell, specifically via an ipsilateral connection.

These results are consistent with anatomy studies which show that the BLA sends primarily glutamatergic efferents to the NAc (Kelley et al., 1982, McDonald, 1991, Brog et al., 1993). Previous electrophysiological studies have shown that stimulation of BLA efferents evoke excitatory responses in NAc neurons (O'Donnell and Grace, 1995, Floresco et al., 2001, Charara and Grace, 2003, Ambroggi et al., 2008, McGinty and Grace, 2008). However, the differentiation between core and shell neural responses in our study is somewhat surprising, as the BLA projects to both the core and shell (McDonald, 1991, Brog et al., 1993, Shinonaga et al., 1994), although more rostral regions of the BLA appear to project more to the core and caudal regions project to the shell (Shinonaga et al., 1994). It is possible that because our BLA infusions are more rostral than caudal, the differential effect of BLA inactivation on DS-evoked firing within the NAc is due to lack of manipulation of shell-mediated projections. This is unlikely however, as the location of our BLA manipulations within the rostral-caudal gradient still contain significant overlap in core and shell projections, particularly in medial core regions where most of our recordings were taken. As such, we suggest that these data provide evidence that contributions of the BLA to NAc core signaling may reflect the behavioral specificity required during our cued-instrumental task. That is, the differential effects of BLA inactivation on NAc cell firing in the core and shell revealed here is consistent with numerous studies that demonstrate functional dissociations between these NAc subregions. Our finding then may reveal a novel neural correlate in the core that is critical in processing discrete reward-predictive stimuli used to guide appetitive responding.

Specifically, transient inactivation of the NAc core attenuates the expression of conditioned approach responses to a CS (Blaiss and Janak, 2009), instrumental conditioned reinforcement (Di Ciano et al., 2008), and cue-induced reinstatement (Fuchs et al., 2004, Floresco et al., 2008). Conversely, the shell appears to have a greater role in suppressing competing responses, independent of discrete cue presentation, as transient inactivation of

the shell decreases conditioned approach to a reward-predictive CS (Blaiss and Janak, 2009) or DS (Ambroggi et al., 2009), but also dramatically increases non-specific approach behavior in response to a non-associated cue (Ambroggi et al., 2009, Blaiss and Janak, 2009). Furthermore, in a cue-reinstatement paradigm, inactivation of the shell can actually enhance cue-induced reinstatement responding indiscriminately across operanda (Floresco et al., 2008). Furthermore, the reported differential contribution of BLA activity to the NAc core is consistent with a growing literature on the amygdalo-striatal network (Cardinal et al., 2002). Specifically, BLA-NAc core interactions have been shown to be critically important to reward processes such as conditioned place preference (Everitt et al., 1991), second-order conditioning (Setlow et al., 2002b, Di Ciano and Everitt, 2004) and stimulus-controlled instrumental responding (Ambroggi et al., 2008).

Although the present findings illustrate the importance of the BLA-NAc core projection in driving cue-evoked responding, there are additional circuits and mechanisms to consider. For example, studies have demonstrated that ventral tegmental area (VTA) inactivation reduces behavioral responding, as well as NAc excitations and inhibitions, evoked by a DS (Yun et al., 2004). Likewise, predictive cues elicit robust phasic dopamine release in the NAc core (Day et al., 2007), and behavioral responding to cues is dopamine dependent (Nicola et al., 2005). Moreover, VTA inactivation also produces a robust decrease in baseline firing rate in NAc neurons, suggesting that tonic firing may be permissive of cue-evoked responses (Yun et al., 2004). In the present study, however, BLA inactivation had no effects on baseline firing rates of NAc core neurons, while significantly reducing DS-evoked excitations. Coupled with the increased latency to behaviorally respond the DS, our results argue that phasic, cue-evoked excitation of NAc core neurons may play a role in driving the behavioral response to cues. This interpretation is further supported by evidence that the magnitude of the phasic DS-evoked excitations in the NAc core predict whether a subsequent behavioral response to the cue is made (Nicola et al., 2004a).

If cue-evoked excitation of NAc core neurons drives cue-evoked responding, it is possible that these responses are also influenced by regions of the prefrontal cortex (PFC). Similar to the BLA, there is a direct excitatory projection from the PFC to the NAc core, descending both ipsilaterally and contralaterally (Sesack et al., 1989, Brog et al., 1993). Neurons in the NAc receive convergent input from the mPFC and the VTA (Sesack and Pickel, 1992). Activity within the PFC is essential for responding to a reward-predictive cue (Ishikawa et al., 2008a), and inactivation of the dorsomedial PFC reduces DS-excitations, as well as inhibitions, in NAc neurons (Ishikawa et al., 2008b). However, large proportions of NAc neurons that are activated by the PFC are also activated by the BLA (O'Donnell and Grace, 1995), and BLA input can directly gate (Goto and O'Donnell, 2002) or indirectly modulate PFC to NAc excitations (McGinty and Grace, 2008). Furthermore, subpopulations of PFC neurons that are responsive to BLA stimulation are also antidromically activated by NAc stimulation, suggesting a polysynaptic pathway via the PFC that may mediate the effects of BLA inactivation on NAc neural activity (Floresco and Tse, 2007). Regardless, it is apparent that convergent excitatory inputs from both the BLA and mPFC, and dopaminergic input from the VTA, are required for activation of NAc core neurons by discrete reward-predictive cues.

Therefore, we propose that a complex neural circuit, wherein converging phasic information from the BLA, PFC and VTA are integrated within the NAc core to influence cue-evoked responding. Phasic dopamine release within the NAc in response to reward-predictive cues is terminally regulated by the BLA (Jones et al., 2009), likely via actions on pre-synaptic glutamate receptors (Floresco et al., 1998, Phillips et al., 2003). Furthermore, concomitant activation of D1 and NMDA receptors in the NAc core is necessary for appetitive instrumental learning (Smith-Roe and Kelley, 2000) and D1 and NMDA receptor activation

is necessary for BLA-induced potentiation of NAc signaling (Floresco et al., 2001). Additionally, recent studies suggest that D1 mediated signals within the NAc core during a cued-discrimination task do not aid in updating the reward-predictive significance of cues, but rather serve to augment instrumental responding (Calaminus and Hauber, 2007). Thus, it is possible that BLA activity in response to reward-predictive cues drives post-synaptic signals within the NAc core, augmenting coincident phasic dopamine signals to amplify neural and behavioral responses to motivationally significant cues.

Acknowledgments

This work was supported by NIH F31 23745 to JLJ and DA 014339 to RMC. The authors thank Lesley Macinnes and Kate Fuhrmann for technical assistance, The Odum Institute for statistical consulting and Brandon J. Aragona, Mitchell F. Roitman and Michael P. Saddoris for helpful discussions.

Abbreviations

ANOVA	analysis of variance
AP	anterior posterior
BLA	basolateral amygdala
BM	baclofen/muscimol cocktail treatment
DS	discriminative stimulus
DV	dorsal-ventral
FR1	fixed-ratio 1 schedule of reinforcement
ML	medial-lateral
NAc	nucleus accumbens
NS	non-associated stimulus
PCA	principal component analysis
PEH	perievent histogram
PFC	prefrontal cortex
VEH	vehicle treatment
VTA	ventral tegmental area

References

Ambroggi, F.; Ghazizadeh, A.; Fields, HL. Separate corticostriatal circuits that promote or inhibit incentive cue responding; 2009 Neuroscience Meeting Planner, vol. Program No. 784.13; Chicago, IL: Society for Neuroscience. 2009; Online

Ambroggi F, Ishikawa A, Fields HL, Nicola SM. Basolateral amygdala neurons facilitate reward-seeking behavior by exciting nucleus accumbens neurons. Neuron. 2008; 59:648–661. [PubMed: 18760700]

Balleine BW, Killcross AS, Dickinson A. The effect of lesions of the basolateral amygdala on instrumental conditioning. J Neurosci. 2003; 23:666–675. [PubMed: 12533626]

Berke JD, Okatan M, Skurski J, Eichenbaum HB. Oscillatory entrainment of striatal neurons in freely moving rats. Neuron. 2004; 43:883–896. [PubMed: 15363398]

Blaiss CA, Janak PH. The nucleus accumbens core and shell are critical for the expression, but not the consolidation, of Pavlovian conditioned approach. Behavioural brain research. 2009; 200:22–32. [PubMed: 19159648]

Brog JS, Salyapongse A, Deutch AY, Zahm DS. The patterns of afferent innervation of the core and shell in the “accumbens” part of the rat ventral striatum: immunohistochemical detection of retrogradely transported fluoro-gold. J Comp Neurol. 1993; 338:255–278. [PubMed: 8308171]

Calaminus C, Hauber W. Intact discrimination reversal learning but slowed responding to reward-predictive cues after dopamine D1 and D2 receptor blockade in the nucleus accumbens of rats. Psychopharmacology. 2007; 191:551–566. [PubMed: 17021925]

Cardinal RN, Parkinson JA, Hall J, Everitt BJ. Emotion and motivation: the role of the amygdala, ventral striatum, and prefrontal cortex. Neurosci Biobehav Rev. 2002; 26:321–352. [PubMed: 12034134]

Carelli RM. Activation of accumbens cell firing by stimuli associated with cocaine delivery during self-administration. Synapse (New York, NY. 2000; 35:238–242.

Carelli RM. Nucleus accumbens cell firing and rapid dopamine signaling during goal-directed behaviors in rats. Neuropharmacology. 2004; 47(Suppl 1):180–189. [PubMed: 15464136]

Carelli RM, Deadwyler SA. Cellular mechanisms underlying reinforcement-related processing in the nucleus accumbens: electrophysiological studies in behaving animals. Pharmacology, biochemistry, and behavior. 1997; 57:495–504.

Carelli RM, Ijames SG, Crumling AJ. Evidence that separate neural circuits in the nucleus accumbens encode cocaine versus “natural” (water and food) reward. J Neurosci. 2000; 20:4255–4266. [PubMed: 10818162]

Carelli RM, Williams JG, Hollander JA. Basolateral amygdala neurons encode cocaine self-administration and cocaine-associated cues. J Neurosci. 2003; 23:8204–8211. [PubMed: 12967981]

Charara A, Grace AA. Dopamine receptor subtypes selectively modulate excitatory afferents from the hippocampus and amygdala to rat nucleus accumbens neurons. Neuropsychopharmacology. 2003; 28:1412–1421. [PubMed: 12799620]

Corbit LH, Balleine BW. Double dissociation of basolateral and central amygdala lesions on the general and outcome-specific forms of pavlovian-instrumental transfer. J Neurosci. 2005; 25:962–970. [PubMed: 15673677]

Corbit LH, Muir JL, Balleine BW. The role of the nucleus accumbens in instrumental conditioning: Evidence of a functional dissociation between accumbens core and shell. J Neurosci. 2001; 21:3251–3260. [PubMed: 11312310]

Day JJ, Roitman MF, Wightman RM, Carelli RM. Associative learning mediates dynamic shifts in dopamine signaling in the nucleus accumbens. Nature neuroscience. 2007; 10:1020–1028.

Day JJ, Wheeler RA, Roitman MF, Carelli RM. Nucleus accumbens neurons encode Pavlovian approach behaviors: evidence from an autoshaping paradigm. The European journal of neuroscience. 2006; 23:1341–1351. [PubMed: 16553795]

Di Ciano P, Everitt BJ. Direct interactions between the basolateral amygdala and nucleus accumbens core underlie cocaine-seeking behavior by rats. J Neurosci. 2004; 24:7167–7173. [PubMed: 15306650]

Di Ciano P, Robbins TW, Everitt BJ. Differential effects of nucleus accumbens core, shell, or dorsal striatal inactivations on the persistence, reacquisition, or reinstatement of responding for a drug-paired conditioned reinforcer. Neuropsychopharmacology. 2008; 33:1413–1425. [PubMed: 17712353]

Everitt, B.; Cardinal, R.; Hall, J.; Parkinson, J.; Robbins, T. Differential involvement of amygdala subsystems in appetitive conditioning and drug addiction. In: Aggleton, J., editor. The Amygdala: A functional analysis. Oxford University Press; Oxford: 2000. p. 353-390.

Everitt BJ, Cador M, Robbins TW. Interactions between the amygdala and ventral striatum in stimulus-reward associations: studies using a second-order schedule of sexual reinforcement. Neuroscience. 1989; 30:63–75. [PubMed: 2664555]

Everitt BJ, Morris KA, O’Brien A, Robbins TW. The basolateral amygdala-ventral striatal system and conditioned place preference: further evidence of limbic-striatal interactions underlying reward-related processes. Neuroscience. 1991; 42:1–18. [PubMed: 1830641]

Everitt BJ, Parkinson JA, Olmstead MC, Arroyo M, Robledo P, Robbins TW. Associative processes in addiction and reward. The role of amygdala-ventral striatal subsystems. Ann N Y Acad Sci. 1999; 877:412–438. [PubMed: 10415662]

Floresco SB, Blaha CD, Yang CR, Phillips AG. Dopamine D1 and NMDA receptors mediate potentiation of basolateral amygdala-evoked firing of nucleus accumbens neurons. J Neurosci. 2001; 21:6370–6376. [PubMed: 11487660]

Floresco SB, McLaughlin RJ, Haluk DM. Opposing roles for the nucleus accumbens core and shell in cue-induced reinstatement of food-seeking behavior. Neuroscience. 2008; 154:877–884. [PubMed: 18479836]

Floresco SB, Tse MT. Dopaminergic regulation of inhibitory and excitatory transmission in the basolateral amygdala-prefrontal cortical pathway. J Neurosci. 2007; 27:2045–2057. [PubMed: 17314300]

Floresco SB, Yang CR, Phillips AG, Blaha CD. Basolateral amygdala stimulation evokes glutamate receptor-dependent dopamine efflux in the nucleus accumbens of the anaesthetized rat. Eur J Neurosci. 1998; 10:1241–1251. [PubMed: 9749778]

Fuchs RA, Evans KA, Parker MC, See RE. Differential involvement of the core and shell subregions of the nucleus accumbens in conditioned cue-induced reinstatement of cocaine seeking in rats. Psychopharmacology (Berl). 2004; 176:459–465. [PubMed: 15138757]

Fuchs RA, Feltenstein MW, See RE. The role of the basolateral amygdala in stimulus-reward memory and extinction memory consolidation and in subsequent conditioned cued reinstatement of cocaine seeking. The European journal of neuroscience. 2006; 23:2809–2813. [PubMed: 16817884]

Ghitza UE, Fabbricatore AT, Prokopenko VF, West MO. Differences between accumbens core and shell neurons exhibiting phasic firing patterns related to drug-seeking behavior during a discriminative-stimulus task. J Neurophysiol. 2004; 92:1608–1614. [PubMed: 15152017]

Ghods-Sharifi S, St Onge JR, Floresco SB. Fundamental contribution by the basolateral amygdala to different forms of decision making. J Neurosci. 2009; 29:5251–5259. [PubMed: 19386921]

Hollander JA, Carelli RM. Cocaine-associated stimuli increase cocaine seeking and activate accumbens core neurons after abstinence. J Neurosci. 2007; 27:3535–3539. [PubMed: 17392469]

Humphries MD, Prescott TJ. The ventral basal ganglia, a selection mechanism at the crossroads of space, strategy, and reward. Progress in neurobiology. 2009

Ishikawa A, Ambroggi F, Nicola SM, Fields HL. Contributions of the amygdala and medial prefrontal cortex to incentive cue responding. Neuroscience. 2008a; 155:573–584. [PubMed: 18640246]

Ishikawa A, Ambroggi F, Nicola SM, Fields HL. Dorsomedial prefrontal cortex contribution to behavioral and nucleus accumbens neuronal responses to incentive cues. J Neurosci. 2008b; 28:5088–5098. [PubMed: 18463262]

Johnson AW, Gallagher M, Holland PC. The basolateral amygdala is critical to the expression of pavlovian and instrumental outcome-specific reinforcer devaluation effects. J Neurosci. 2009; 29:696–704. [PubMed: 19158296]

Jones JL, Day JJ, Aragona BJ, Wheeler RA, Wightman RM, Carelli RM. Basolateral Amygdala Modulates Terminal Dopamine Release in the Nucleus Accumbens and Conditioned Responding. Biological psychiatry. 2009

Kelley AE, Domesick VB, Nauta WJ. The amygdalostriatal projection in the rat--an anatomical study by anterograde and retrograde tracing methods. Neuroscience. 1982; 7:615–630. [PubMed: 7070669]

McDonald AJ. Topographical organization of amygdaloid projections to the caudatoputamen, nucleus accumbens, and related striatal-like areas of the rat brain. Neuroscience. 1991; 44:15–33. [PubMed: 1722890]

McDonald RJ, White NM. A triple dissociation of memory systems: hippocampus, amygdala, and dorsal striatum. Behavioral neuroscience. 1993; 107:3–22. [PubMed: 8447956]

McFarland K, Kalivas PW. The circuitry mediating cocaine-induced reinstatement of drug-seeking behavior. J Neurosci. 2001; 21:8655–8663. [PubMed: 11606653]

McGinty VB, Grace AA. Selective activation of medial prefrontal-to-accumbens projection neurons by amygdala stimulation and Pavlovian conditioned stimuli. Cereb Cortex. 2008; 18:1961–1972. [PubMed: 18065719]

McLaughlin RJ, Floresco SB. The role of different subregions of the basolateral amygdala in cue-induced reinstatement and extinction of food-seeking behavior. Neuroscience. 2007; 146:1484–1494. [PubMed: 17449185]

Murray EA. The amygdala, reward and emotion. Trends in cognitive sciences. 2007; 11:489–497. [PubMed: 17988930]

Nicola SM. The nucleus accumbens as part of a basal ganglia action selection circuit. Psychopharmacology (Berl). 2007; 191:521–550. [PubMed: 16983543]

Nicola SM, Taha SA, Kim SW, Fields HL. Nucleus accumbens dopamine release is necessary and sufficient to promote the behavioral response to reward-predictive cues. Neuroscience. 2005; 135:1025–1033. [PubMed: 16165291]

Nicola SM, Yun IA, Wakabayashi KT, Fields HL. Cue-evoked firing of nucleus accumbens neurons encodes motivational significance during a discriminative stimulus task. J Neurophysiol. 2004a; 91:1840–1865. [PubMed: 14645377]

Nicola SM, Yun IA, Wakabayashi KT, Fields HL. Firing of nucleus accumbens neurons during the consummatory phase of a discriminative stimulus task depends on previous reward predictive cues. Journal of neurophysiology. 2004b; 91:1866–1882. [PubMed: 14645378]

O'Donnell P, Grace AA. Synaptic interactions among excitatory afferents to nucleus accumbens neurons: hippocampal gating of prefrontal cortical input. J Neurosci. 1995; 15:3622–3639. [PubMed: 7751934]

Ostlund SB, Balleine BW. Differential involvement of the basolateral amygdala and mediodorsal thalamus in instrumental action selection. J Neurosci. 2008; 28:4398–4405. [PubMed: 18434518]

Parkinson JA, Olmstead MC, Burns LH, Robbins TW, Everitt BJ. Dissociation in effects of lesions of the nucleus accumbens core and shell on appetitive pavlovian approach behavior and the potentiation of conditioned reinforcement and locomotor activity by D-amphetamine. J Neurosci. 1999; 19:2401–2411. [PubMed: 10066290]

Parkinson JA, Robbins TW, Everitt BJ. Dissociable roles of the central and basolateral amygdala in appetitive emotional learning. Eur J Neurosci. 2000; 12:405–413. [PubMed: 10651899]

Paton JJ, Belova MA, Morrison SE, Salzman CD. The primate amygdala represents the positive and negative value of visual stimuli during learning. Nature. 2006; 439:865–870. [PubMed: 16482160]

Paxinos, G.; Watson, C. The rat brain in stereotaxic coordinates. El Sevier; New York: 2005.

Peoples LL, Uzwiak AJ, Gee F, West MO. Operant behavior during sessions of intravenous cocaine infusion is necessary and sufficient for phasic firing of single nucleus accumbens neurons. Brain Res. 1997; 757:280–284. [PubMed: 9200758]

Phillips AG, Ahn S, Howland JG. Amygdalar control of the mesocorticolimbic dopamine system: parallel pathways to motivated behavior. Neurosci Biobehav Rev. 2003; 27:543–554. [PubMed: 14599435]

Roesch MR, Singh T, Brown PL, Mullins SE, Schoenbaum G. Ventral striatal neurons encode the value of the chosen action in rats deciding between differently delayed or sized rewards. J Neurosci. 2009; 29:13365–13376. [PubMed: 19846724]

Saddoris MP, Gallagher M, Schoenbaum G. Rapid associative encoding in basolateral amygdala depends on connections with orbitofrontal cortex. Neuron. 2005; 46:321–331. [PubMed: 15848809]

Sesack SR, Deutch AY, Roth RH, Bunney BS. Topographical organization of the efferent projections of the medial prefrontal cortex in the rat: an anterograde tract-tracing study with Phaseolus vulgaris leucoagglutinin. The Journal of comparative neurology. 1989; 290:213–242. [PubMed: 2592611]

Sesack SR, Pickel VM. Prefrontal cortical efferents in the rat synapse on unlabeled neuronal targets of catecholamine terminals in the nucleus accumbens septi and on dopamine neurons in the ventral tegmental area. The Journal of comparative neurology. 1992; 320:145–160. [PubMed: 1377716]

Setlow B, Gallagher M, Holland PC. The basolateral complex of the amygdala is necessary for acquisition but not expression of CS motivational value in appetitive Pavlovian second-order conditioning. The European journal of neuroscience. 2002a; 15:1841–1853. [PubMed: 12081664]

Setlow B, Holland PC, Gallagher M. Disconnection of the basolateral amygdala complex and nucleus accumbens impairs appetitive pavlovian second-order conditioned responses. Behavioral neuroscience. 2002b; 116:267–275. [PubMed: 11996312]

Setlow B, Schoenbaum G, Gallagher M. Neural encoding in ventral striatum during olfactory discrimination learning. Neuron. 2003; 38:625–636. [PubMed: 12765613]

Shinonaga Y, Takada M, Mizuno N. Topographic organization of collateral projections from the basolateral amygdaloid nucleus to both the prefrontal cortex and nucleus accumbens in the rat. Neuroscience. 1994; 58:389–397. [PubMed: 8152545]

Simmons DA, Neill DB. Functional interaction between the basolateral amygdala and the nucleus accumbens underlies incentive motivation for food reward on a fixed ratio schedule. Neuroscience. 2009; 159:1264–1273. [PubMed: 19344638]

Smith-Roe SL, Kelley AE. Coincident activation of NMDA and dopamine D1 receptors within the nucleus accumbens core is required for appetitive instrumental learning. J Neurosci. 2000; 20:7737–7742. [PubMed: 11027236]

Taha SA, Fields HL. Encoding of palatability and appetitive behaviors by distinct neuronal populations in the nucleus accumbens. J Neurosci. 2005; 25:1193–1202. [PubMed: 15689556]

Tye KM, Cone JJ, Schairer WW, Janak PH. Amygdala neural encoding of the absence of reward during extinction. J Neurosci. 30:116–125. [PubMed: 20053894]

Tye KM, Janak PH. Amygdala neurons differentially encode motivation and reinforcement. J Neurosci. 2007; 27:3937–3945. [PubMed: 17428967]

Yun IA, Wakabayashi KT, Fields HL, Nicola SM. The ventral tegmental area is required for the behavioral and nucleus accumbens neuronal firing responses to incentive cues. J Neurosci. 2004; 24:2923–2933. [PubMed: 15044531]

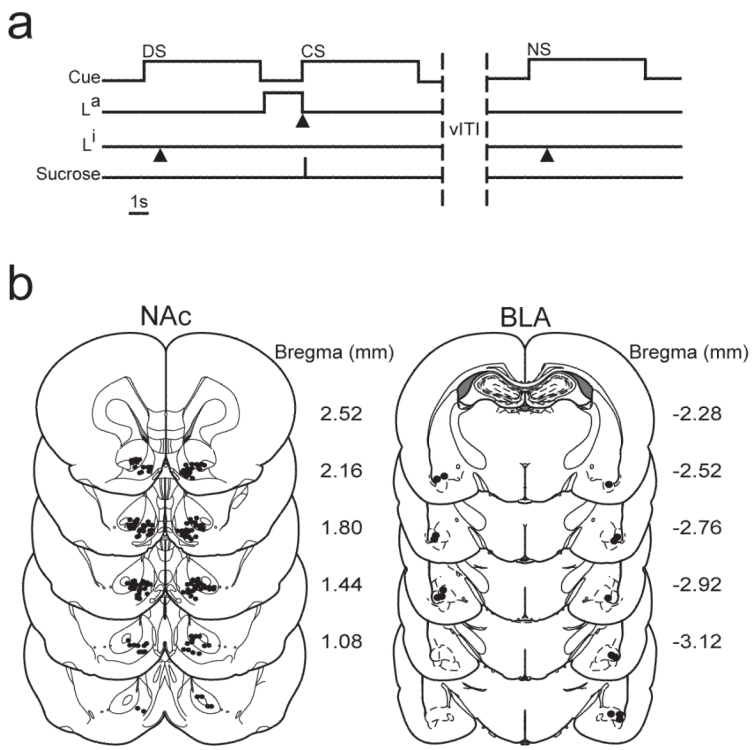

Figure 1.

a) Schematic of the operant task. During sessions, one of two trials was presented, the DS or NS. The DS was presented for 6s, after which the active lever (L^a) was extended. Responses on the L^a resulted in sucrose delivery and CS onset (6s). Responses during the NS had no programmed consequences. The inactive lever (L^i) was always present. Black triangles denote a lever response. b) Histological representation of electrode and cannula placement. Left diagrams show the NAc placements of electrodes at recording. Right diagrams illustrate the tip of the microinjector placed into the BLA cannula. Images are adapted from (Paxinos and Watson, 2005).

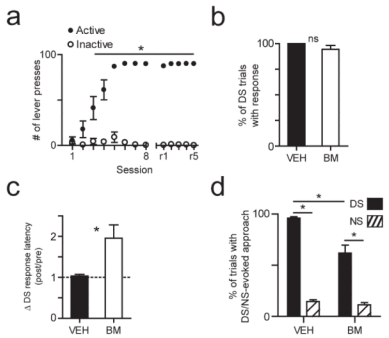

Figure 2.

Conditioned responding following BLA treatment. a) Average number of lever presses across the final eight training sessions and subsequent retraining days. b) Average percentage of DS trials with an active lever response following BLA treatment. c) The average change in DS response latency following BLA treatment. d) The average percentage of trials with a DS- or NS-evoked approach following BLA treatment. Data and error bars reflect mean ± SEM. ns denotes $p>0.05$; * denotes $p<0.05$.

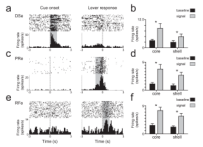

Figure 3.

A subset of NAc neurons in the core and shell exhibit phasic excitations in cell firing relative to cue onset or the lever press response. a) PEH and raster display show the activity of a representative DSe neuron; activity is aligned to DS-onset (left panel; dotted line) or the lever press response (right panel; dotted lined). DSe epoch (signal period) is denoted by the gray bar. b) Average firing rate across baseline and signal periods for all DSe neurons in the core and shell. c) PEH and raster display show the activity of representative PRe neuron; activity aligned to DS-onset (left panel; dotted line) or the lever press (right panel; dotted lined). PRe epoch (signal period) is denoted by the gray bar. d) Average firing rate during the baseline and signal periods for all PRe neurons in the core and shell. e) PEH and raster display show activity of a representative RFe neuron; firing aligned to DS-onset (left panel; dotted line) or operant response (right panel; dotted lined). RFe epoch (signal period) is denoted by the gray bar. f) Average firing rate during the baseline and signal periods for all RFe neurons in the core and shell. Data and error bars reflect mean ± SEM. * denotes $p<0.01$.

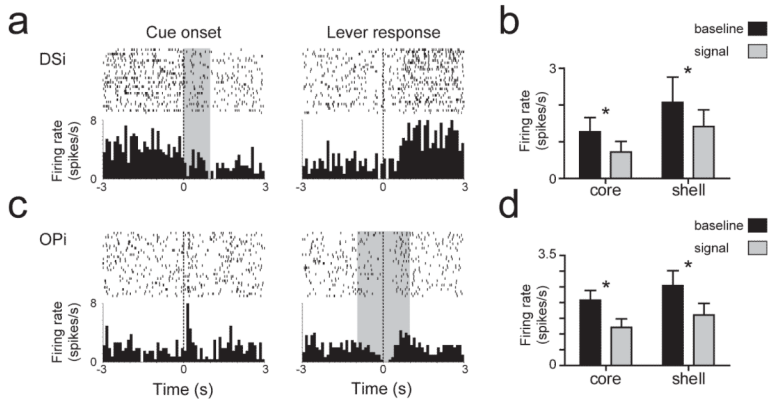

Figure 4.

Another subset of NAc neurons (types DSi and OPi) show phasic inhibitions in cell firing relative to cue onset or the lever press response in the core and shell. a) PEH and raster display of a representative DSi neuron aligned to DS-onset (left panel; dotted line) or the lever press (right panel; dotted lined). DSi epoch (signal period) is denoted by the gray bar. b) Average baseline and signal firing rates for all DSi neurons in the core and shell. c) PEH and raster display showing the activity of a representative OPi neuron aligned to DS-onset (left panel; dotted line) or operant response (right panel; dotted lined). OPi epoch (signal) is denoted by the gray bar. d) Average baseline and signal firing rate for all OPi neurons in the core and shell. Data and error bars reflect mean ± SEM. * denotes $p<0.01$.

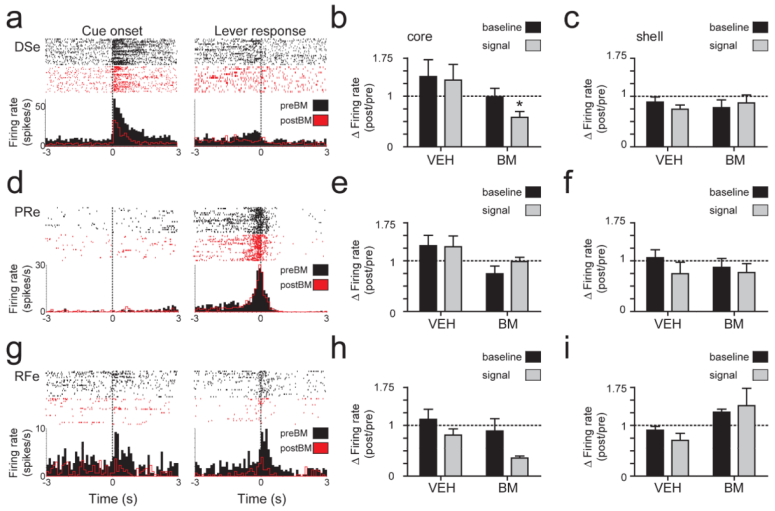

Figure 5.

Effects of BLA inactivation on NAc neurons exhibiting phasic excitations (types DSe, PRe and RFe). a) PEH and raster displays show the activity of a representative DSe neuron in the NAc core before (black) and following (red) BM treatment aligned to DS-onset (left panel; dotted line) and the lever press response (right panel; dotted lined). Average change (defined as POST firing rate/PRE firing rate) in baseline and signal firing rates for all DSe neurons in the core (b) and shell (c) following vehicle (VEH) or BM treatment. d) PEH and raster display show the activity of a representative PRe neuron in the core before (black) and following (red) BM treatment aligned to cue-onset (left panel; dotted line) and the lever response (right panel; dotted lined). Average change in baseline and signal firing rates for all PRe neurons in the core (e) and shell (f) following VEH or BM treatment. g) PEH and raster showing example RFe core neuron before (black) and following (red) BM treatment aligned to cue-onset (left panel; dotted line) and lever response (right panel; dotted lined). Average change baseline and signal firing rates for all in RFe cells in the core (h) and shell (i) following VEH or BM treatment. Data and error bars reflect mean ± SEM. * denotes $p<0.05$.

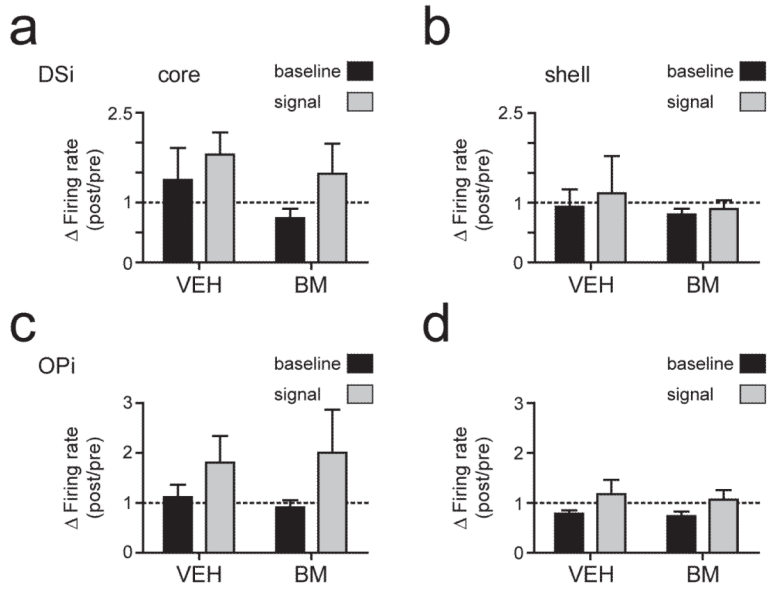

Figure 6.

Effects of BLA inactivation on NAc neurons exhibiting phasic inhibitions (types DSi and OPi). Average change in baseline and signal firing rates across all DSi neurons in the core (a) and shell (b). Average change in baseline and signal firing rates across all OPi neurons in the core (c) and shell (d). Data and error bars reflect mean ± SEM.

Table 1

Neural responses from a single session

			Core	n=66	Shell	n=60
Neural response		**Analysis window**	***n***	**% total**	***n***	**% total**
DS	e	0-1s post DS	12	18.2	7	11.7
	i	0-1s post DS	13	19.7	11	18.3
NS	e	0-1s post NS	9	13.6	4	6.7
	i	0-1s post NS	7	9.1	6	10.0
Pre-response	e	0-1s before lever press	18	27.3	8	13.3
	i	0-1s before lever press	17	25.8	18	30.0
Post-response	e	0-1s after lever press	28	42.4	21	35.0
	i	0-1s after lever press	24	36.4	19	31.7

The data were taken from the first VEH recording session from each animal. The percentages within the table are based on the number of neurons recorded from each subregion (*n*=66 core; *n*=60 shell; *n*=126 total). Of the 126 neurons, 108 exhibited phasic activity (i.e. at least one of the given response profiles).

Table 2

Mean (±SEM) firing rate (spikes/s) of phasic NAc core neurons during ipsilateral BLA manipulation

Treatment	VEH					BM				
Epoch		Baseline		Signal			Baseline		Signal	
Cell Type	*n*	PRE	POST	PRE	POST	*n*	PRE	POST	PRE	POST
DSe *** †	6	2.22 ± 0.57	3.41 ± 1.3	7.06 ± 3.03	9.7 ± 4.80	7	1.93 ± 0.78	1.6 ± 0.69	6.88 ± 3.78	5.09 ± 3.65
PRe †	12	1.38 ± 0.3	2.16 ± 0.76	6.33 ± 1.88	8.65 ± 2.64	7	2.70 ± 0.83	1.83 ± 0.70	9.83 ± 3.57	9.42 ± 3.26
RFe #†	9	2.77 ± 0.74	3.01 ± 0.83	6.74 ± 1.01	5.76 ± 1.37	4	1.63 ± 1.01	1.03 ± 0.36	5.29 ± 2.01	1.79 ± 0.59
DSi †	7	1.14 ± 0.52	1.20 ± 0.47	0.82 ± 0.45	1.02 ± 0.38	6	1.75 ± 0.81	1.30 ± 0.67	1.85 ± 1.27	1.35 ± 0.66
OPi †	19	1.84 ± 0.37	1.85 ± 0.42	1.15 ± 0.37	1.21 ± 0.35	12	2.48 ± 0.61	1.94 ± 0.58	0.94 ± 0.35	0.72 ± 0.25

Remaining effects $p>0.05$

*** $p<0.05$ epoch x infusion x treatment

\# $p<0.05$ epoch x infusion

† $p<0.05$ epoch

Table 3

Mean (±SEM) firing rate (spikes/s) of phasic NAc shell neurons during ipsilateral BLA manipulation

Treatment	VEH					BM				
Epoch		Baseline		Signal			Baseline		Signal	
Cell Type	*n*	PRE	POST	PRE	POST	*n*	PRE	POST	PRE	POST
DSe †	4	2.40 ± 1.18	2.13 ± 1.08	4.67 ± 1.65	3.42 ± 1.19	4	4.98 ± 1.70	3.37 ± 1.31	7.53 ± 1.90	6.07 ± 1.89
PRe #†	5	1.60 ± 0.77	1.59 ± 0.67	4.22 ± 1.24	3.30 ± 1.18	8	4.03 ± 0.99	3.29 ± 0.92	7.67 ± 1.85	5.53 ± 1.41
RFe †	7	2.09 ± 0.54	1.78 ± 0.42	5.77 ± 1.66	4.12 ± 1.30	3	1.64 ± 0.93	2.12 ± 1.27	6.87 ± 4.87	7.87 ± 4.4
DSi †	6	2.49 ± 1.20	1.43 ± 0.54	1.69 ± 0.78	1.06 ± 0.43	8	3.94 ± 0.95	3.23 ± 0.97	3.10 ± 0.85	2.48 ± 0.64
OPi #†	16	2.46 ± 0.55	1.74 ± 0.37	1.40 ± 0.37	0.91 ± 0.24	12	2.83 ± 0.82	1.99 ± 0.62	1.24 ± 0.34	1.17 ± 0.34

Remaining effects $p>0.05$

# $p<0.05$ epoch x infusion

† $p<0.05$ epoch